Interpretation of growth, mortality, and recruitment patterns in size-at-age, growth increment, and size frequency data

Barry D. Smith and Louis W. Botsford

Abstract: The determination of age structure for many invertebrate populations is often difficult because individuals lack the hard body parts that record growth (e.g., otoliths, scales), and population size distributions often lack patterns expressing an age structure. Consequently, assessments of invertebrate fisheries are often of necessity length-based. Here we review the quantitative basis for inferring life-history characteristics such as growth and mortality rates from size frequency distributions that do not necessarily exhibit age pulses. We use an equilibrium solution to the von Foerster equation to describe the dependence of size distributions and optimal lower size limits for harvest on life-history characteristics. We then describe various forms of the von Bertalanffy growth model that include stochasticity in different ways, and the patterns of size versus age, growth increment versus size and time-at-large, and numbers versus size to which the different models lead. We show how our portrayals can help an analyst develop a general intuitive basis for visual interpretation of size-related patterns of growth and mortality in their data by formally analysing size frequency and growth data from a few typical invertebrate populations.

Résumé : La détermination de la structure d'âge de nombreuses populations d'invertébrés est souvent difficile parce que ces organismes ne possèdent pas de structures corporelles dures qui permettent d'enregistrer la croissance (p. ex. otolithes ou écailles) et parce que, souvent, les distributions de tailles de la population ne montrent pas de caractéristiques permettant d'exprimer la structure d'âge. Par conséquent, les évaluations des pêcheries d'invertébrés sont souvent, par nécessité, fondées sur la longueur des organismes. Dans la présente communication, nous passons en revue les fondements quantitatifs permettant de déduire des caractéristiques du cycle vital comme les taux de croissance et de mortalité à partir des distributions de fréquences de tailles qui ne présentent pas nécessairement de pointes liées à l'âge. Nous utilisons une solution d'équilibre à l'équation de von Foerster pour décrire la dépendance, à l'égard des caractéristiques du cycle vital, des distributions de taille et des limites de taille inférieure optimales pour la récolte. Nous décrivons ensuite diverses formes du modèle de croissance de von Bertallanffy qui tiennent compte de la stochasticité de différentes façons; nous décrivons également les caractéristiques taille selon l'âge, augmentation de croissance selon la taille et la période en liberté et effectifs selon la taille, auxquelles mènent les différents modèles. Nous montrons comment nos caractérisations peuvent aider un analyste à développer une base intuitive générale pour l'interprétation visuelle des caractéristiques de croissance et de mortalité liées à la taille dans leurs données en analysant formellement les données sur la croissance et la fréquence de tailles tirées de quelques populations d'invertébrés typiques. [Traduit par la Rédaction]

Introduction

Even the most basic of population assessments require information on the growth and mortality rates of individuals in a population (Ricker 1975; Gulland 1983). Size-at-age data have typically been used to provide growth information since growth is a measure of change in size over time. Since high quality size-at-age and numbers-at-age data are often difficult to acquire for invertebrates, invertebrate fisheries usually cannot be assessed using techniques such as virtual population analysis (VPA, Pope 1972) and its descendants (see Hilborn and Walters 1992) which are often applied to fish. Size frequency analysis is often the best alternate methodology for estimating growth and mortality when individuals do not have permanent anatomical structures which record the passage of time.

Recruitment pulses in a size frequency distribution can aid visual and analytic interpretation of year-class patterns for temperate species undergoing continuous growth (Schnute and Fournier 1980; Smith and McFarlane 1990; Botsford et al. 1994). The growth and mortality processes can be visualized as the dissipation of recruitment pulses through time (Fournier and Breen 1983). A conceptually and analytically more challenging problem is the interpretation of growth and mortality rates from size frequency distributions which lack multiple age pulses. Such distributions would be typical of species which tend not to have annual recruitment pulses, but which have

B.D. Smith.[1] Department of Fisheries and Oceans, Maurice Lamontagne Institute, P.O. Box 1000, Mont-Joli, QC G5H 3Z4 Canada.

L.W. Botsford. Department of Wildlife, Fish and Conservation Biology, University of California, Davis, CA 95616, U.S.A.

Correct citation: Smith, B.D., and Botsford, L.W. 1998. Interpretation of growth, mortality, and recruitment patterns in size-at-age, growth, increment, and size frequency data. *In* Proceedings of the North Pacific Symposium on Invertebrate Stock Assessment and Management. *Edited by* G.S. Jamieson and A. Campbell. Can. Spec. Publ. Fish. Aquat. Sci. 125. pp. 125–139.

[1]Present address: Environment Canada - Canadian Wildlife Service, Pacific Wildlife Research Centre, 5421 Robertson Road, Delta, BC V4K 3N2, Canada.

individuals recruiting at a constant rate into the population of interest. In temperate climates recruitment pulses are generally seasonal and are apparent for the smaller individuals in size distributions. When growth is asymptotic the pulses tend to become smeared at larger sizes due to growth variability (Botsford et al. 1994). In contrast, tropical and subtropical species are more likely to be characterized by size frequency distributions lacking age pulses.

A size frequency distribution provides static information on the size composition of a population. If there are no age pulses, then the distribution will be only qualitatively informative about growth, mortality, and recruitment. However, size-at-age and growth increment information, i.e., that obtained from a laboratory growth study, or a field mark–recapture study, can be quantitatively informative about growth rates. When such growth information (i.e., from individuals) is combined with size frequency data (population aggregate information) together they can be quantitatively informative about growth and mortality rates for a population. Our intention with this paper is to inform readers (*i*) of what visual inspection of size frequency distributions qualitatively can tell us about the relationship between growth and mortality for a population, and (*ii*) what visual inspection of size-at-age and growth increment plots qualitatively can tell us about growth and growth variability for a population.

The mathematical framework upon which we develop our concepts of growth and mortality also provides the basis for a general methodology for analyzing size frequency data and growth increment data in combination to measure growth and mortality, and for calculating an optimal minimum size limit. The methodologies for analyzing growth increment and size frequency data are separable thereby allowing the growth increment analysis to be linked to an analysis of size frequency data characterized by either constant or pulsed (i.e., age-structured) recruitment. The details (including precision, bias, and robustness to assumptions) of formal parameter estimation appear in other papers such as Smith and McFarlane (1990) and Smith et al. (1998) where we apply our models to the particular problems of assessing the population dynamics of the lingcod (*Ophiodon elongatus*) in British Columbia, and the red sea urchin (*Strongylocentrotus franciscanus*) in California.

Size frequency distributions

We need a formal basis upon which to build a model for size frequency distributions based on growth and mortality functions of size. The von Foerster size-structured equation (von Foerster 1959; Van Sickle 1977; DeAngelis and Mattice 1979; Huston and DeAngelis 1987) provides the basis for describing how the density of individuals in a population changes over time. We present it here as

$$[1] \quad \frac{\partial n(l,t)}{\partial t} = -\frac{\partial}{\partial l}[n(l,t)g(l)] - D(l)n(l,t)$$

where $n(l, t)$ is the density of individuals of size l at time t, $g(l)$ is the growth rate of an individual of size l, and $D(l)$ is the mortality rate of a individual of size l (see Table 1 for symbol definitions). As shown in Botsford et al. (1994) we can obtain a density expression for a size frequency distribution under steady-state and constant recruitment conditions by setting $\partial n(l, t)/\partial t = 0$ which yields

$$[2] \quad \frac{\partial n(l)}{\partial l} = -\frac{n(l)}{g(l)}\left[\frac{\partial g(l)}{\partial l} + D(l)\right]$$

Equation 2 thus describes the size-based steady-state density of numbers-at-size for any size frequency distribution. A representation such as eq. 2 would be valid for interpreting size frequencies which appear not to change appreciably in form over time. The convenience of eq. 2 is that it allows an analyst to explore the consequences of various size-dependent functions of growth, $g(l)$, and mortality, $D(l)$. If we assume von Bertalanffy growth then

$$[3] \quad g(l) = K'(L - l)$$

As an extension of eq. 3 we let K' represent $K + bl$ below (and in Figs. 1 and 2) and choose a form of von Bertalanffy growth that allows K' to change with size l,

$$[4] \quad g(l) = (K + bl)(L - l)$$

with

$$[5] \quad \frac{\partial g(l)}{\partial l} = -K + b(L - 2l)$$

(Note that the equivalent of eq. 5 in Table 1 of Botsford et al. (1994) contains a sign error.) The advantage of eq. 4 is its potential to generate a sigmoidal growth curve when $b > 0$. (We recognize, however, that other functional forms, e.g., Richards, logistic, have a similar ability.)

We therefore have

$$[6] \quad \frac{\partial n(l)}{\partial l} = -\left[\frac{-K + b(L - 2l) + D(l)}{(K + bl)(L - l)}\right] n(l)$$

if we define $D(l)$ as positive. Equation 6 can be readily integrated numerically over size l to generate a size frequency distribution.

The general (non-steady-state) solution to eq. 2 is

$$[7] \quad n(l, t) = R[t - A(l)]\frac{g(l_*)}{g(l)}\, e^{-\int_{l_*}^{l} [D(l')/g(l')]\, \partial l'}$$

(Banks et al. 1991). $R[t - A(l)]$ represents the time varying recruitment flux, $n(l_*, t - A(l))g(l_*)$, across the recruitment boundary l_* for an individual of length l and age $A(l)$. If, for example, we retain the mortality rate constant over size (i.e., $D(l) = Z$) and assume growth according to eq. 4, then the following analytical solution exists:

$$[8] \quad n(l, t) = R[t - A(l)]\left(\frac{L - l}{L - l_*}\right)^{[Z/(K+bL)]-1}\left(\frac{K + bl_*}{K + bl}\right)^{[Z/(K+bL)]+1}$$

If growth is simplified to be strictly von Bertalanffy, i.e., $b = 0$ then

$$[9] \quad n(l, t) = R[t - A(l)]\left(\frac{L - l}{L - l_*}\right)^{(Z/K)}$$

If recruitment is assumed to be a constant value R, then the dependencies on time t and age-at-size $A(l)$ can be dropped. Analytical solutions are rare for models where mortality is a function of size, e.g.,

$$[10] \quad D(l) = Z\, e^{-cl}$$

Table 1. Definitions for variables appearing in this paper.

Symbol	Definition
	time
	size
	the size in a size frequency distribution to which individuals first recruit
	size when fully exploited yield-per-recruit is maximized
	deterministic asymptotic size for an individual
	represents $K + bl$
	deterministic instantaneous rate of change in growth rate for an individual
	shape parameter for a modified von Bertalanffy or Richards growth function
	density of individuals in a size distribution
	recruitment rate
	growth rate at size l
	mortality rate at size l
	natural mortality rate at size $l = 0$
	l-dependent mortality coefficient
μ_L	mean of L for a population
σ_L^2	variance of L for a population
μ_K	mean of K for a population
σ_K^2	variance of K for a population
A	age
A_0	age at $l = 0$ in size-at-age data
A_0'	age at $l = 0$ in size frequency data
μ_A	expected size-at-age A
σ_A^2	expected variance in sizes-at-age A
ϕ_A	in size frequency data, the deviation of the mean of an age pulse from that predicted by a growth function
$V_l(l)$	variance of measurement error at size l
T	time period over which growth increments are measured
μ_l	expected growth increment at size l during time T
σ_l^2	variance in growth increments at size l during time T
$w(l)$	weight-at-size l
φ	scaling parameter of weight-at-size function
ν	power parameter of weight-at-size function
$E[\bullet]$	expected value of the bracketed quantity
$V[\bullet]$	variance of the bracketed quantity

with $c > 0$. For such models we rely on numerical solutions to the differential equations to generate a corresponding size frequency distribution.

An analogy of eq. 9 has previously appeared in the literature accompanied with a discussion of its implications for the shape of a size frequency distribution (Barry and Tegner 1990). Other authors have exploited the benefit of knowing the ratio Z/K for interpreting fish population dynamics (see Pauly 1984; Pauly and Morgan 1987) or using size data to interpret mortality rates (Ebert 1973; Van Sickle 1977; Fournier and Breen 1983). Here we extend these interpretations by showing that eqs. 2 and 7 coupled with independent stochastic variability in von Bertalanffy's K and L parameters (Sainsbury 1980) have a particular ability to be informative of the underlying growth and mortality functions that give observed size frequency distributions their characteristic equilibrium shapes. These equations also form the basis for analytical models which facilitate estimation of stochastic growth and deterministic mortality parameters from size frequency, size-at-age and growth increment data (Smith and McFarlane 1990; Smith et al. 1998).

To appreciate the utility of these models observe that eq. 2 has special diagnostic value in that for deterministic growth and mortality $\partial n(l)/\partial l$ will equal zero when $\partial g(l)/\partial l = -D(l)$. Immediately this gives us a tool for visually assessing size frequency distributions then interpreting the underlying population dynamics, i.e., a plateau in the size distribution will occur when $\partial g(l)/\partial l + D(l) = 0$. Deterministic and stochastic portrayals of distributions arising from these models appear in Fig. 1 with the corresponding values for the derivative of the growth rate, $-\partial g(l)/\partial l$, and the mortality rate, $D(l)$, appearing in Fig. 2. For example (Figs. 1*a* Deterministic, 2*a*), von Bertalanffy growth and a constant mortality rate with $D(l) = Z = K$, generates a plateau that occurs over the entire domain of l.

In Fig. 1 we have admitted variability in von Bertalanffy's asymptotic size L by allowing L to be a normally distributed random variable with a mean of μ_L and variance $\sigma_L 2$ (Sainsbury 1980). We have not admitted variability in von Bertalanffy's K because it has little discernible effect on an equilibrium size distribution (Botsford et al. 1994). Although no single model should be considered a unique or even biologically precise descriptor of growth, we found Sainsbury's

Fig. 1. Characteristic size frequency distributions under the constant recruitment assumption. For all examples $\sigma_K = 0$ because they are indistinguishable from otherwise similar size frequency plots with $\sigma_K > 0$ (Botsford et al. 1994). Histograms represent a random sample (n = 1000) of the analytical stochastic distribution organized into 5 unit cells. The parameter values for each plot are as follows: (*a*) $\mu_L = 100$, $\sigma_L = 0$, $\mu_K = 0.3$, $b = 0$, $D(l) = 0.3$; (*b*) $\mu_L = 100$, $\sigma_L = 10$, $\mu_K = 0.3$, $b = 0$, $D(l) = 0.1$; (*c*) $\mu_L = 100$, $\sigma_L = 10$, $\mu_K = 0.1$, $b = 0$, $D(l) = 0.3$; (*d*) $\mu_L = 100$, $\sigma_L = 10$, $\mu_K = 0.1$, $b = 0$, $D(l) = 4.0e^{-0.051}$; and (*e*) $\mu_L = 100$, $\sigma_L = 10$, $\mu_K = 0.3$, $b = 0.005$, $D(l) = 0.1$.

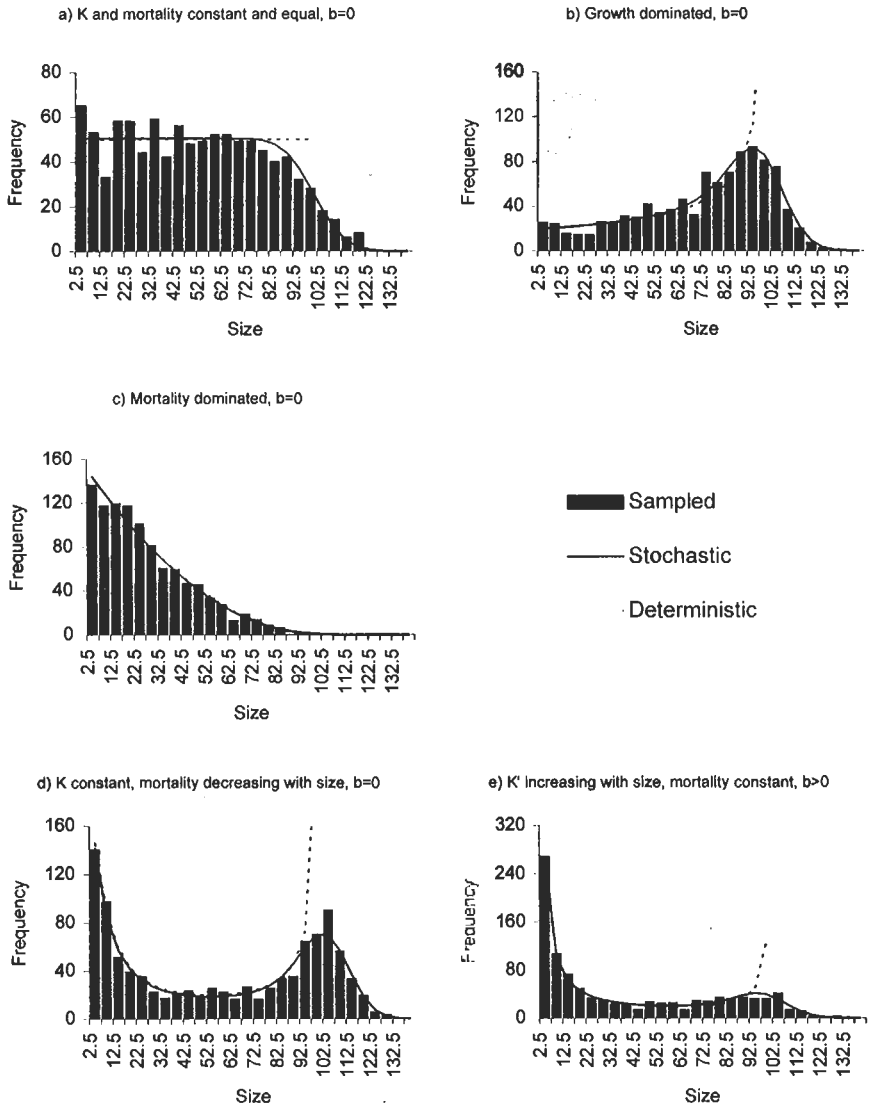

(1980) model to be particularly useful for describing stochastic growth as it is expressed in size frequency distributions, size-at-age data, and growth increment data that we have seen. This stochastic parameterization of growth overcomes the incompatibility of deterministic von Bertalanffy functions representing size-at-age data and growth increment data that was highlighted by Francis (1988).

We refer to Figs. 1*b* (with $\mu_k > Z$) and 1*c* (with $\mu_k < Z$) as growth-dominated and mortality-dominated distributions, respectively. If either $\partial g(l)/\partial l$ or $D(l)$ vary with length then there is potential for distributional forms more interesting than these. Distributions with a pronounced mode near the maximum size of individuals in the distribution appear frequently in nature as either a growth-dominated or bimodal distributional form. Figures 1*d* and 1*e* show that both

$\partial g(l)/\partial l = -K$, with $D(l) = Z\,e^{-cl}$ (Figs. 1*d* and 2*d*)

and $\partial g(l)/\partial l = -K + b(L - 2l)$, with $D(l) = Z$ (Figs. 1*e* and 2*e*)

can produce a bimodal distribution. In both cases the peak of the right-hand mode tends to occur near the value for μ_L with the spread around μ_L giving an indication of the value of σ_L. Note that the portrayals in Fig. 1 are ideal and natural distributions are not likely to perfectly conform to those distributions. In particular, size selectivity during data collection will result in the smallest individuals being under-represented in the distribution.

At least two recruitment processes can complicate the size distributions portrayed in Fig. 1. Periodic pulsed recruitment can introduce age pulses into a distribution thus disguising the underlying growth and mortality patterns that are more evident

Fig. 2. Functions of size for $-\partial g(l)/\partial l$ and $D(l)$ for the characteristic size frequency distributions portrayed in Fig. 1. In the deterministic case a plateau in a size frequency distribution will occur when $-\partial g(l)/\partial l = D(l)$.

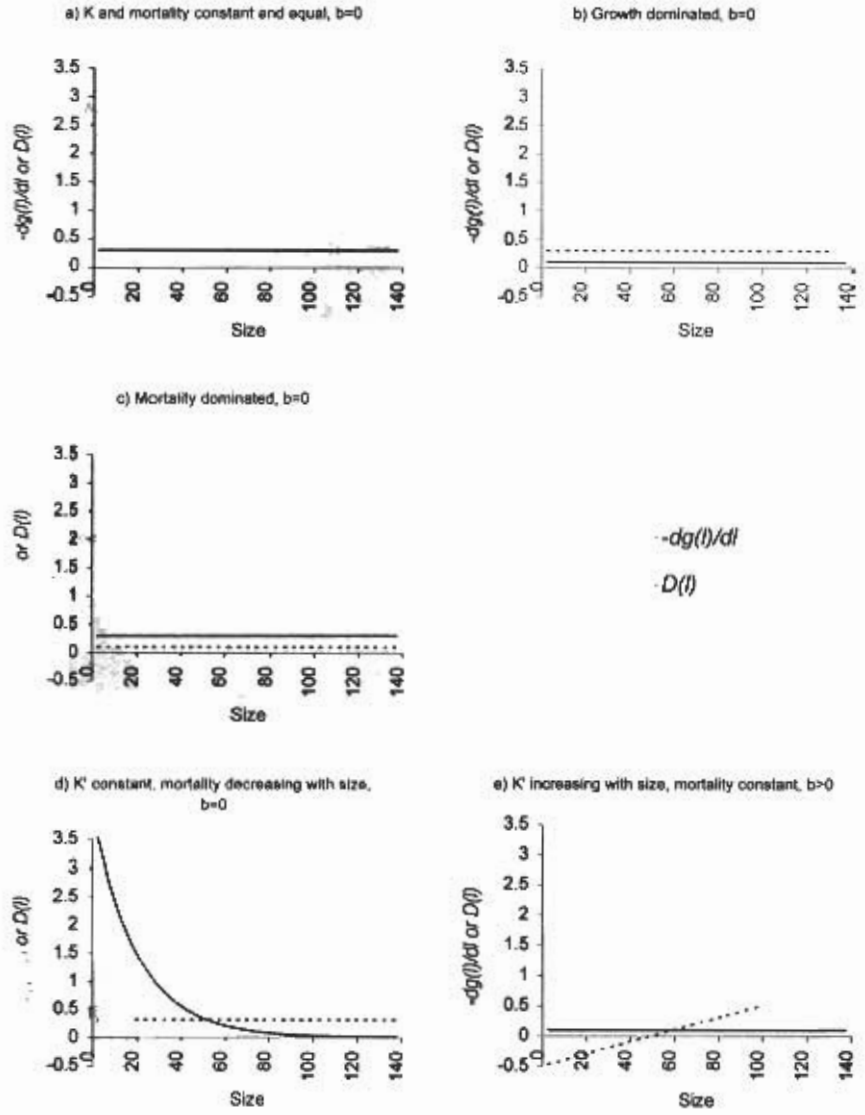

in the constant recruitment situation. Periodic pulses will introduce age pulses into a size distribution which will shift toward the right over time, tending to result in a repetition of the size distribution pattern annually if annual recruitment is somewhat constant (Fig. 3). Random recruitment pulses occurring in a population where recruitment is typically low, but which occasionally experiences a strong recruitment event, can lead an analyst to suspect regular recruitment pulses as in Fig. 3 unless a time series of collected distributions indicates a pattern of random recruitment (Fig. 4).

Only repeated sampling over time can resolve whether the nature of recruitment into size frequency distributions is regular or random. In principle, random recruitment such as that portrayed in Fig. 4 would be describable by a probability function. As yet we know of no analytical models for estimating growth and mortality parameters from size frequency distributions characterized by random recruitment. However, simulation studies have shown (Smith et al. 1998) that if the magnitude of recruitment variability is low, say a coefficient of variation (RV) of two or less, then growth and mortality parameters can be confidently measured from such distributions.

Maximizing yield-per-recruit

Having a simple method to calculate the maximum yield-per-recruit from size frequency data is valuable since, due to a paucity of fishery data, many invertebrate fisheries are passively managed by minimum size limits, or area and seasonal closures (see Jamieson 1986). Our model facilitates a simple calculation for determining a minimum size limit (l_x) that would maximize yield-per-recruit if it is assumed that virtually all individuals above l_x are rapidly exploited by a fishery.

For species that are candidates to be managed by a minimum size limit, and for which the instantaneous fishing mortality (Ricker 1975) can be assumed to approach infinity, i.e., a 100% exploitation rate above the minimum size l_x, maximum yield-per-recruit occurs when the value of l_x maximizes the function $n(l)g(l)w(l)$. The per-recruit flux, $n(l_x)g(l_x)$, across the

Fig. 3. Size frequency distributions characterizing pulsed recruitment for the mortality-dominated and growth-dominated examples of Fig. 1. The winter and summer portrayals depict the shift to the right of pulses for a species whose peak in annual recruitment occurs in summer. For all examples $\sigma_K = 0$, $b = 0$, $c = 0$. Histograms represent a random sample ($n = 1000$) of the analytical stochastic distribution organized into 5 unit cells. The parameter values for each plot are as follows: (*a* and *b*) $\mu_L = 100$, $\sigma_L = 10$, $\mu_K = 0.1$, $D(l) = 0.3$; and (*c* and *d*) $\mu_L = 100$, $\sigma_L = 10$, $\mu_K = 0.3$, $D(l) = 0.1$.

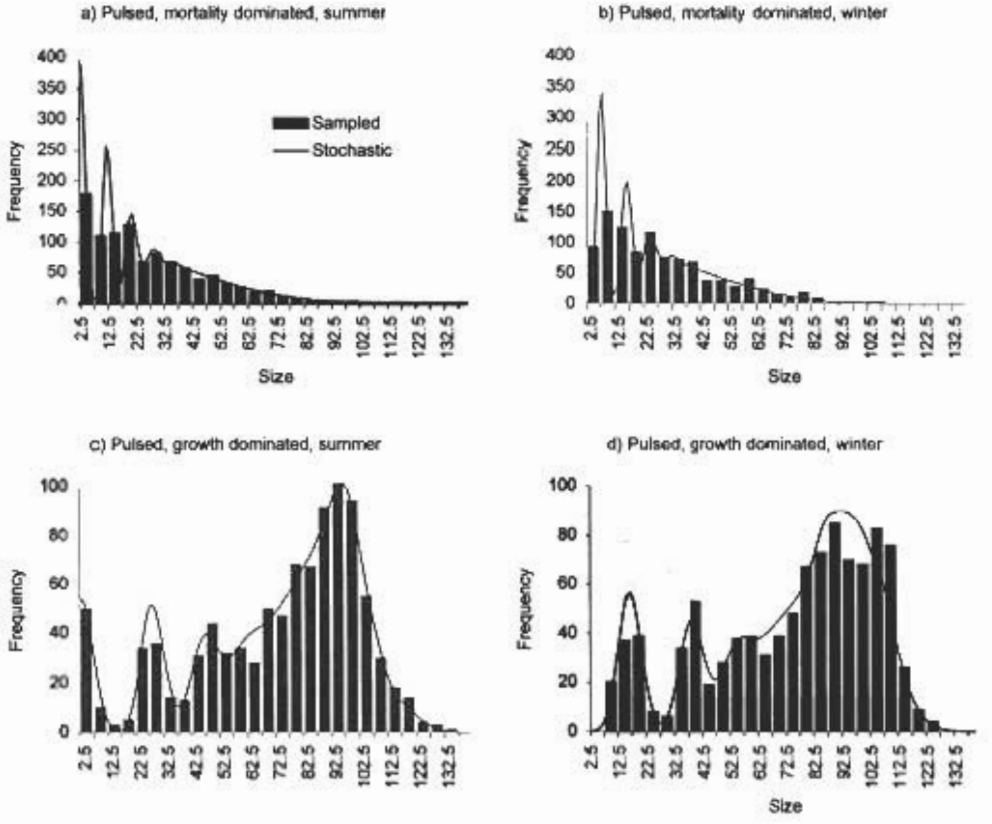

minimum size boundary l_x is converted to biomass from numbers by $w(l_x)$. The function $w(l)$ thus relates yield in weight to a linear measure of size by, for example, a power model as in $w(l) = \varphi l^{\nu}$. Typically $w(l)$ would represent total weight, but in some cases, such as that of the red sea urchin, it could represent gonad weight since gonad flesh is the commercial product.

The estimate for the size l_x ($l_x > 0$) when fully exploited yield-per-recruit is maximized is obtained by solving

$$[11] \quad \frac{\partial[n(l)\, g(l)\, w(l)]}{\partial l} = 0$$

which simplifies to

$$[12] \quad 0 = g(l_x) \left.\frac{\partial w(l)}{\partial l}\right|_{l=l_x} - w(l_x)\, D(l_x)$$

Equation 12 depends neither on population density, $n(l)$, nor recruitment history $R[t - A(l)]$ and therefore can be applied to populations without having concern about past recruitment patterns. It is noteworthy that l_x is inherently conservative. That is, if the population of interest actually experienced an exploitation rate less than 100%, when managed by a minimum size limit of l_x, then yield-per-recruit would be maximized at a size smaller than l_x.

For von Bertalanffy growth and constant mortality, Z, maximum fully exploited yield-per-recruit occurs when

$$[13] \quad l_x = \frac{L}{\left(+\frac{Z}{K\nu}\right)}$$

if yield in weight is related to a linear measure of size by the power parameter ν. Equation 13 bears resemblance to Hoenig's (1987) function to estimate the size when the surplus yield in numbers (i.e., $\nu = 1$) of a population is optimized. When growth is considered to be stochastic in L and K as above, then the necessary condition for the l_x that produces maximum yield is

$$[14] \quad 0 = E\,[g(l_x)] \left.\frac{\partial w(l)}{\partial l}\right|_{l=l_x} - w(l_x)\, D(l_x$$

Continuing with the previous example, the independence of L and K leads to

$$[15] \quad l_x = \frac{\mu_L}{\left(1 + \frac{Z}{\mu_K \nu}\right)}$$

Solutions to Eq. 14 are less tractable if $g(l)$ includes power

Fig. 4. Characteristic growth-dominated size frequency distributions with random recruitment. Each figure (*a–d*) portrays 30 realizations (thin lines) of the analytical deterministic distribution (thick line) when random variation in recruitment is added. Fig. 4*a* portrays 30 realizations of a random sample ($n = 1000$) of the analytical stochastic distribution organized into 5 unit cells when the coefficient of variation of recruitment (RV) is zero. The other examples (*b–d*) use a value of RV = 5. The value for RV is the coefficient of variance for a lognormal probability distribution of recruitment over monthly time cells. For all examples $\mu_L = 100$, $\sigma_L = 10$, and $\sigma_K = 0$. Note that the ratio μ_K/Z determines the analytical shape of the size distribution.

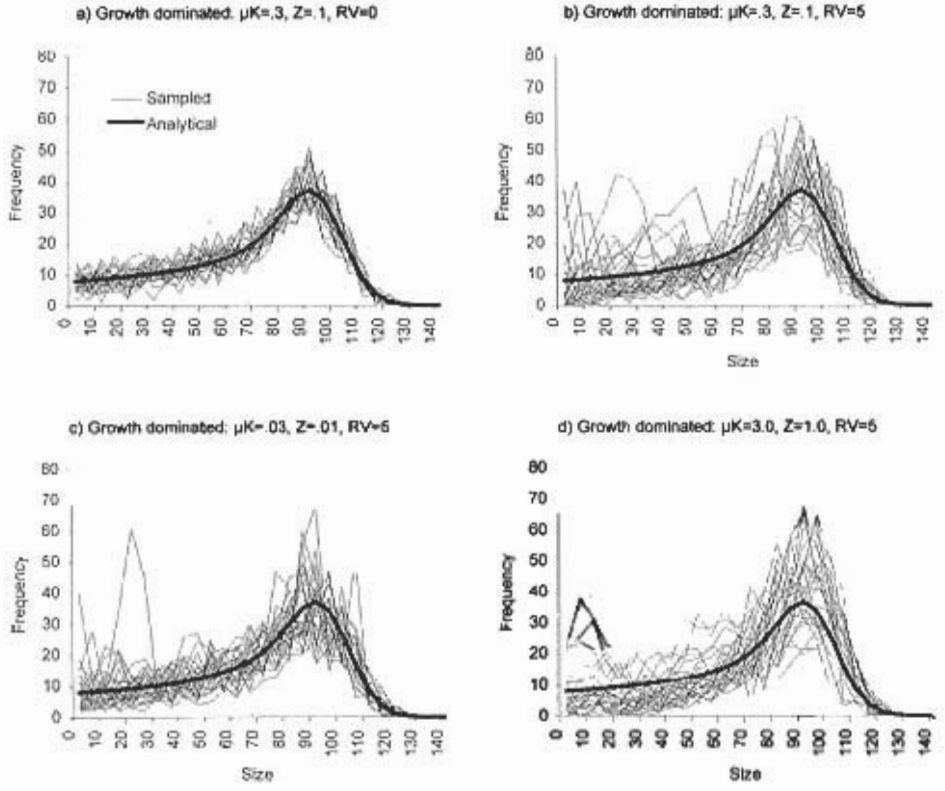

parameters such as in the Richards function (see Schnute 1981),

$$[16]\quad E[g(l)] = E\left[\frac{K\,l}{b}\left(\left(\frac{L}{l}\right)^{b}\right)\right]$$

however, it would probably be acceptable to assume $E[L^b] = E[L]^b$ in the above case knowing that the coefficient of variance of L is likely to be quite small, say about 10%.

It is noteworthy that the value of l_x depends only on the ratio Z/K, but the value for the maximum harvest depends on $g(l)$. For example, the expected size distributions for the populations portrayed in Fig. 4 are identical because all four distributions are characterized by the same ratio Z/K, and will thus have the same value for l_x. However the individuals in the population represented by Fig. 4*d* grow 100× faster, i.e., individuals move much more quickly from the left to the right of the size frequency distribution, than those in Fig. 4*c*. Although the calculated value for l_x would be the same in all cases, the expected yield, $\int n(l)g(l)w(l)\partial t$, from the population in Fig. 4*c* would be only 1% of that for the population represented in Fig. 4*d*, given the same constant recruitment rate, R, and value of v.

Size-at-age data

The stochastic von Bertalanffy growth (eq. 4) model already discussed can generate graphical representations for size-at-age which allow analysts to interpret the growth model generating their observed data. By using μ_A and $\sigma_A 2$ to represent the mean size-at-age and variance-at-age, respectively, the distributions in Figs. 5*a–5d*, when $b = 0$, can be generated by

$$[17]\quad \mu_A = \mu_L(1 - E[e^{-\mu_K(A-A_0)}])$$

$$[18]\quad \sigma_A^2 = \eta\,\sigma_L^2 + \mu_L^2\,V[e^{-\mu_K(A-A_0)}] + V_f(l)$$

where

$$[19]\quad E[e^{-\mu_K(A-A_0)}] = \left(+\frac{(A-A_0)\,\sigma_K^2}{\mu_K}\right)^{-\frac{\mu_K^2}{\sigma_K^2}}$$

$$[20]\quad V[e^{-\mu_K(A-A_0)}] = \left(+\frac{2(A-A_0)\,\sigma_K^2}{\mu_K}\right)^{-\frac{\mu_K^2}{\sigma_K^2}} - \left(1+\frac{(A-A_0)\,\sigma_K^2}{\mu_K}\right)^{-\frac{2\mu_K^2}{\sigma_K^2}}$$

and

Fig. 5. Characteristic size-at-age plots. The corresponding growth increment plots for a time-at-large of one age unit appear in Fig. 6. The parameter values for each plot are as follows: (*a*) μ_L=100, σ_L= 10, μ_K= 0.3, σ_K= 0, b = 0; (*b*) μ_L= 100, σ_L= 0, μ_K= 0.3, σ_K= 0.1, b = 0; (*c* and *d*) μ_L= 100, σ_L= 10, μ_K= 0.3, σ_K= 0.1, b = 0; and (*e*) μ_L= 100, σ_L= 10, μ_K= 0.01, σ_K= 0.0033, b = 0.005.

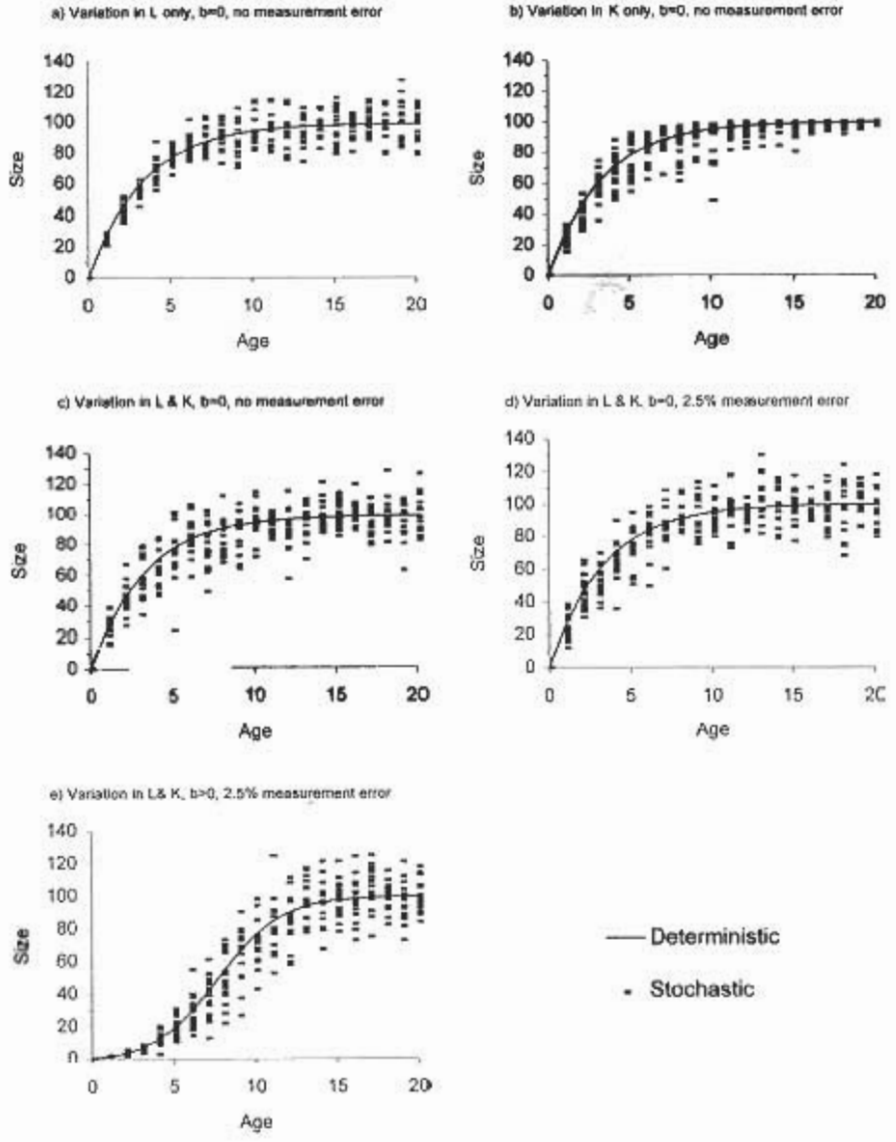

$$[21]\quad \eta = 1 - 2\left(1 + \frac{(A - A_0)\,\sigma_K^2}{\mu_K}\right)^{-\frac{\mu_K^2}{\sigma_K^2}} + \left(1 + \frac{2(A - A_0)\,\sigma_K^2}{\mu_K}\right)^{-\frac{\mu_K^2}{\sigma_K^2}}$$

(Sainsbury 1980; Smith and McFarlane 1990) where A is the age of an individual and A_0 is the age when the expected size of an individual is zero. The term $V_l(l)$ represents the variance of error in the measurement of size l as a function of size.

Note that the deterministic solution to the growth model of eq. 4 ($b > 0$) as a function of age is

$$[22]\quad l = \frac{L\,K(1 - e^{-(K+bL)(A-A_0)})}{L\,b\,e^{-(K+bL)(A-A_0)} + K}$$

Owing to its complexity there exist no simple analytical stochastic expressions for expected sizes-at-age, growth increments, and their variances for this growth model; rather we calculate these values numerically.

Figures 5*a*, 5*b*, and 5*c* ($b = 0$) distinctly portray the variation in L, K, or both in size-at-age data. Species expressing variance in L only will produce size-at-age distributions that will tend to increase in variance with increasing size. Species expressing variance in K only will tend to grow toward a singular value for L. Variance in size-at-age will be maximum at intermediate ages. Species expressing variance in both variables will display a maximum variance in size-at-age at intermediate sizes. Error in the measurement of size is also not discernible in size-at-age plots (e.g., compare Fig. 5*c* with 5*d*). If $b > 0$, then the same arguments with regard to variance in L and K apply as with $b = 0$, however, the sigmoidal form of the size-at-age curve is readily apparent (Fig. 5*e*).

Fig. 6. Characteristic growth increment plots. The corresponding size-at-age plots appear in Fig. 5. The parameter values for each plot are as follows: (*a*) $\mu_L = 100$, $\sigma_L = 10$, $\mu_K = 0.3$, $\sigma_K = 0$, $b = 0$; (*b*) $\mu_L = 100$, $\sigma_L = 0$, $\mu_K = 0.3$, $\sigma_K = 0.1$, $b = 0$; (*c* and *d*) $\mu_L = 100$, $\sigma_L = 10$, $\mu_K = 0.3$, $\sigma_K = 0.1$, $b = 0$; and (*e*) $\mu_L = 100$, $\sigma_L = 10$, $\mu_K = 0.01$, $\sigma_K = 0.0033$, $b = 0.005$.

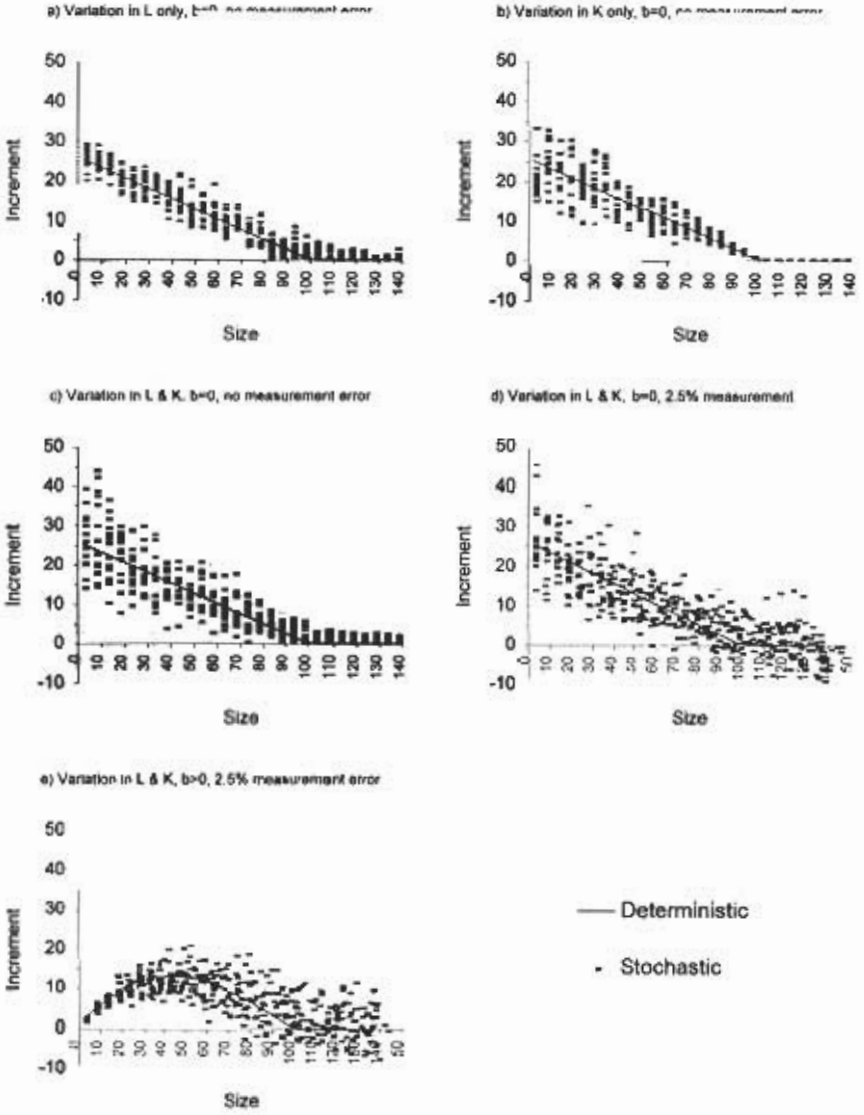

Growth increment data

Analogous growth increment plots (Fig. 6) exist for each of the five size-at-age distributional forms of Fig. 5. The patterns in Fig. 6 are generated by the following growth increment models (eqs. 23 and 24), with $b = 0$, (Sainsbury 1980; Smith and McFarlane 1990) where T is the elapsed time between an initial, then subsequent, size measurement to determine growth. We use μ_l and $\sigma_l 2$ to represent the mean growth increment and the variance of growth increments, respectively, conditional on the initial size l of an individual and the time period T.

$$[23] \quad \mu_l = (\mu_L - l)(1 - E[e^{-\mu_K T}])$$

$$[24] \quad \sigma_l^2 = \eta\, \sigma_L^2 + (\mu_L - l)^2\, V[e^{-\mu_K T}] + V_f(l)$$

In eqs. 23 and 24 $E[e^{-\mu_K T}]$, $V[e^{-\mu_K T}]$, and η are as in eqs. 19–21 but with $A - A_0$ replaced by T.

Growth increments for a species with growth variance only in L (i.e., $\sigma_L > 0$, $\sigma_K = 0$) will generate a growth increment plot that tends to have constant variance-at-size over sizes considerably smaller than μ_L (Fig. 6*a*). As size approaches the domain of the distribution of L's, the lower growth rate limit of zero begins to affect the form of the distribution of increments-at-size causing the variance of increments-at-size to decrease. If there is variance only in K (i.e., $\sigma_L = 0$, $\sigma_K > 0$) then a growth increment plot will have a conical shape with a vertex at μ_L (Fig. 6*b*). Growth increments plots expressing variance in both L and K will display decreasing variance with size but not to a vertex as in the case with $\sigma_K = 0$ (Fig. 6*c*). Additionally, the occurrence of negative growth increments in such a plot is direct evidence of measurement error $V_f(l)$ when it is known that individuals of the species in question cannot undergo negative growth (Fig. 6*d*). As previously mentioned, such direct evidence will not be distinguishable in a plot of size-at-age (Fig. 5). A sigmoidal growth form ($b > 0$) would introduce

Fig. 7. Size-at-age (SA, $n = 1108$) and size frequency (SF, $n = 2547$) data for the waved whelk (*Buccinum undatum*) with the corresponding predicted fits using each data set independently and in combination. The parameter values corresponding to the fits to these data are in Table 2.

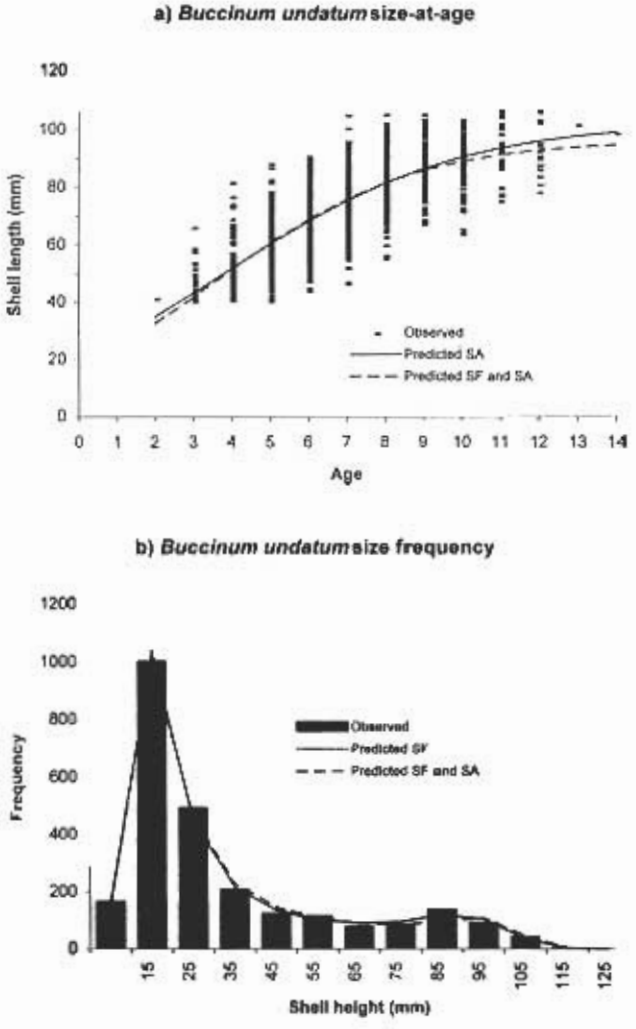

distinct convex curvature into the growth increment plot as in Fig. 6*e*.

Constant recruitment examples

Buccinum undatum

For our first example using real data we present a size-at-age (SA) plot (Fig. 7*a*) for the waved whelk (*Buccinum undatum*) from the Gulf of St. Lawrence (Gendron 1992 and Louise Gendron, Maurice Lamontagne Institute (MLI), unpublished data). Age was determined by interpreting growth annuli on an individual whelk's operculum. The absence of the smallest individuals in Fig. 7*b* is due to SCUBA divers choosing not to sample such small individuals for age analysis. Notwithstanding that individuals less than 40 mm shell length were not sampled, we can interpret from this plot that a stochastic sigmoidal growth form could adequately describe growth for this species. A corresponding size frequency (SF) plot of shell length constructed from measurements of individuals exhaustively sampled from quadrats placed on a sand-mud bottom (Jalbert et al. 1989) indicates a possible bimodal form (Fig. 7*b*), with the absence of the smallest individuals in the distribution resulting from the inability to quantitatively sample the smallest individuals.

If we assume that the left-hand mode in Fig. 7*b* is composed of several age-classes which show no apparent pattern of interannual recruitment variability, then we might interpret that recruitment in the waved whelk occurs at a relatively constant rate. Thus growth and mortality for the waved whelk can be described by growth and mortality processes leading to bimodality in an equilibrium size distribution as depicted in Figs. 1*e*, 2*e*, and 5*e*. However, the assumption of constant recruitment could later be falsified if size frequency plots collected sequentially in time portray a progression of year-classes.

The size-at-age data and size frequency data (Figs. 7*a* and 7*b*) appear to be in accordance with each other (Table 2). Note particularly that formal statistical analyses of these size-at-age and size frequency data seem to indicate a value for a μ_L near 90–103 mm shell length with a value for the standard deviation (SD) of L (σ_L) of 6–8 mm shell length. We remind you that size frequency information is uninformative of the SD of K (σ_K) (Fig. 1 and Botsford et al. 1994). Our combined analysis of these size-at-age and size frequency data estimated mortality, $D(l)$, to vary with shell length according to eq. 10. We used eq. 14 and our estimates of growth, $g(l)$, and $D(l)$ to calculate l_x, the shell length when fully exploited meat yield-per-recruit is maximized. Accepting the value of 3.1 for the power parameter v relating meat yield to shell length (L. Gendron, MLI, unpublished data), we estimated l_x to be near 79–82 mm (Table 2).

Strongylocentrotus franciscanus

In our second example, the red sea urchin (*Strongylocentrotus franciscanus*), scrutiny of the size frequency data (SF) in Fig. 8*b* seems to suggest a value for μ_L around 100 mm test diameter. However statistical analysis of the growth increment data alone (GI, Fig. 8*a*) yielded an estimate for μ_L of 71 mm test diameter (Table 2). This seems low in comparison with the size frequency data, but the standard error (SE) of this estimate was 45 mm test diameter. The slope of the relationship between growth increment and initial size, where it is not modified by encroachment upon the domain of L, represents a value of 0.71 yr^{-1} for μ_K (SE: 0.66 yr^{-1}). There is no pattern in the data to indicate the presence of variance in K, (i.e., $\sigma_K = 0$ yr^{-1}). The large standard errors for the growth parameter estimates obtained from these growth increment data indicate they are not particularly informative about growth on their own.

By accepting that negative growth is unlikely since these urchins were well-fed, the negative values for increments are direct evidence of measurement error. Thus the uncertainty in the estimate of μ_L can be explained in part by the measurement error that enters this analysis (about 2.5% of test diameter). The presence of measurement error signifies that individuals repeatedly measured will yield different test diameters. In the case of the red sea urchin this nonrepeatability can arise from irregularities in test diameter, asymmetry of the test and/or imprecise measurements.

Table 2. Formally estimated growth and mortality parameter values associated with the constant recruitment examples.

	Parameter								
	μ_L	σ_L	μ_K	σ_K		A_0	Z	c	υ	l_x
					***Buccinum undatum* (waved whelk)**					
Size-at-age data (SA)	102.8	6.1	1.9×10^{-3}	0*	3.3×10^{-3}	.4				
Size frequency data (SF)	90.1	8.2	2.3×10^{-2}	0*	3.6×10^{-3}		1*	2.6×10^{-2}	3.1	79
Both data sets (SA and SF)	96.5	6.4	2.9×10^{-3}	0*	4.1×10^{-3}	–8.7	0.62	1.5×10^{-2}	3.1	82
					***Strongylocentrotus franciscanus* (red sea urchin)**					
Growth increment data (GI)	71.3	37.6	0.71	0*	0*					
Size frequency data (SF)	111.3	16.2	3.43	0*	0*			0*	3.6	103
Both data sets (GI and SF)	112.2	15.9	0.46	0*	0*	—	0.13	0*	3.6	104
					***Mactromeris polynyma* (Stimpson's surf clam)**					
Growth increment data	70.8	2.8	0.44	0.15	0*					
Size-at-age data (SA)	115.1	5.3	1.2×10^{-2}	0*	1.3×10^{-3}	–6.8				
Size frequency data (SF)	109.0	7.5	0.18	0*	$.6\times10^{-2}$		1*	0*	2.95	90
SA and SF data sets	111.4	6.2	1.9×10^{-2}	0*	$.2\times10^{-3}$	–4.8	0.09	0*	2.95	90

Note: These values are used to calculate the tabled values for l_x. For size frequency (SF) analyses the reported parameter values are accompanied by unreported parameter values for selectivity curves. All size dimensions are millimeters and all time dimensions are years. An asterisk (*) beside a number indicates the number was required to be fixed at that value (e.g., Z) or the number tended toward that boundary value and was subsequently fixed at that value to increase model parsimony. When Z is fixed at one, as it must be for an analysis of size frequency data alone, then μ_K is redefined to represent the ratio μ_K/Z, and b is redefined to represent the ratio b/Z. A dash (—) indicates that the parameter does not play a role in that particular analysis. Plots corresponding to these data are in Figs. 7–9.

The uncertainty in the growth estimates provided by the analysis of the growth increment data alone can be overcome by an analysis of the size frequency and growth increment data in combination. Performing this joint analysis shows that these growth increment data are reasonably compatible with field collected size frequency data (Kalvass et al. 1991; Fig. 8*b*). The analysis of size frequency and growth increment data in combination yielded parameter values ($\mu_L \approx$ 112 mm, $\sigma_L \approx$ 16 mm, $\mu_K = 0.46$ yr^{-1}) which are consistent with the range of possible values yielded by the growth increment data alone.

Since the independent growth increment data provide us with an estimate for the growth rate, $g(l)$, then a value for the mortality rate, $D(l)$, can be obtained by size frequency analysis. For the example portrayed, a constant value for $D(l)$ of 0.13 yr^{-1} was adequate to explain the observed size frequency distribution. If we assume gonad weight is related to test diameter by the power parameter $\nu = 3.6$, then the use of eq. 15 results in an estimate for l_x, the test diameter when fully exploited gonad yield-per-recruit is maximized, of 103–104 mm (Table 2). The value of $\nu = 3.6$ was interpreted from gonad weight versus test diameter data of Tegner and Levin (1983) that had been collected in December at a time when gonads are ripe and the fishery for gonads in southern California was most active (Kato and Schroeter 1985).

Mactromeris polynyma

Laboratory-obtained growth increment data for Stimpson's surf clam (*Mactromeris polynyma*) from the Gulf of St. Lawrence (Fig. 9*b*; Michel Giguère and Jean Lambert, MLI, preliminary and unpublished data) indicate von Bertalanffy growth with a μ_L near 71 mm shell length, a value for σ_L of 3 mm shell length, a value of μ_K near 0.44 yr^{-1}, and significant variance in K (i.e., $\sigma_K = 0.15$ yr^{-1}) (Table 2). In contrast, the size-at-age data (Jean Lambert, MLI, preliminary and unpublished data; Fig. 9*a*) indicate sigmoidal growth with quite different parameter values than for the growth increment data, and no pattern to suggest a value for $\sigma_K > 0$ yr^{-1}. The two forms of growth data are therefore both visually and statistically incompatible. More satisfyingly, the size-at-age and size frequency data appear compatible since they indicate a value for μ_L of about 109–115 mm shell length with a value for σ_L of about 5–8 mm shell length (Table 2). If we accept the parameter values from the joint analysis of the latter two data sets, and use a value for meat yield in relation to shell length of $\upsilon = 2.95$ (Jean Lambert, MLI, unpublished data), then we calculate a value for l_x of 90 mm (Table 2).

The value of finding such discrepancies among data sets is our ability to judge the quality of the data. In this case the conflicting interpretations of the data led the biologist studying

Fig. 8. Growth increment (GI, open circles: $n = 28$, 23 days-at-large; diamonds: $n = 32$, 27 days-at-large) and size frequency (SF, $n = 375$) data for the red sea urchin (*Strongylocentrotus franciscanus*) with the corresponding predicted fits using each data set independently and in combination. The parameter values corresponding to the fits to these data are in Table 2. Note that each series of growth increment data corresponds to a different time-at-large and thus produces its own fit using the same model parameters.

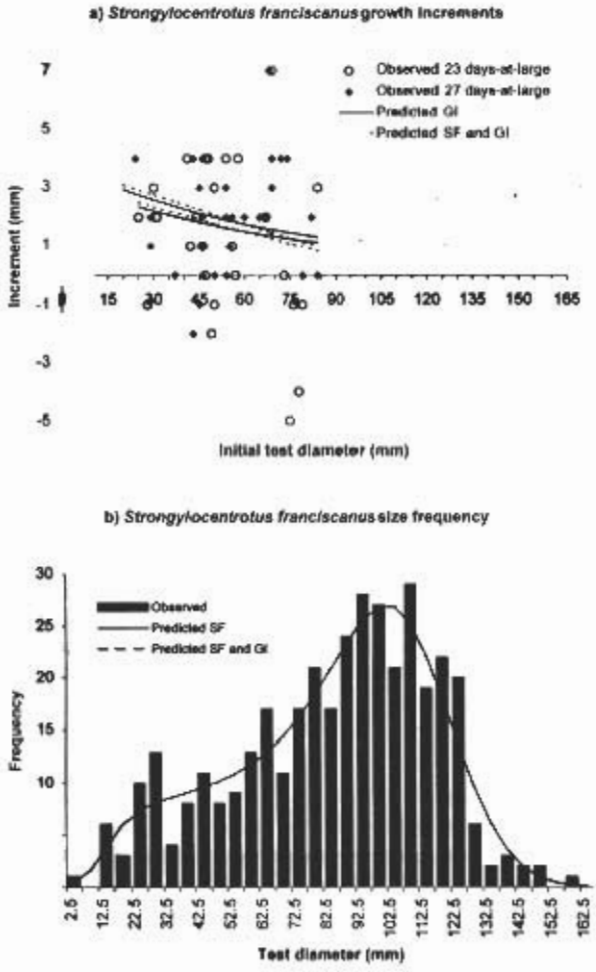

Fig. 9. Size-at-age (SA, $n = 255$), growth increment (GI, $n = 357$, time-at-large is 467 and 474 days) and size frequency (SF, $n = 1770$) data for Stimpson s surf clam (*Mactromeris polynyma*) with the corresponding predicted fits using each data set independently and using the size-at-age and size frequency data in combination. The parameter values corresponding to the fits to these data are in Table 2.

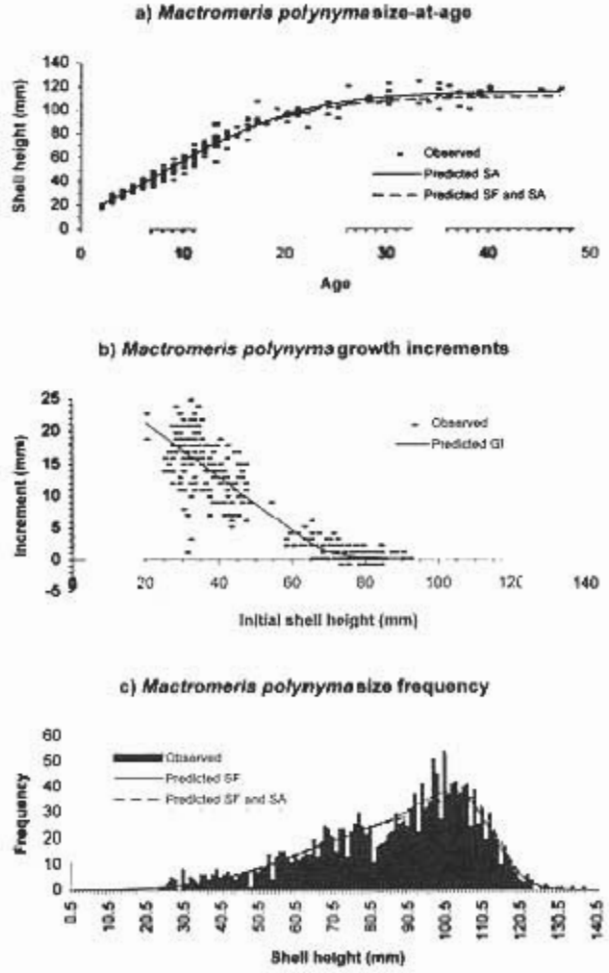

this species to conclude that the laboratory growth experiments were yielding seriously inaccurate growth increment data. His conclusion was partly based on the premise that we should have the most confidence in the size frequency data. These data tend to be least vulnerable to bias since they are collected in the field and are not subject to the unnatural conditions that accompany laboratory experiments, or the uncertainty in accepting growth checks as annuli. His next step was to execute field growth studies that would be more likely to yield growth rates compatible with the field-collected size frequency data.

Pulsed recruitment example

Placopecten magellanicus

We chose size-at-age data (Fig. 10*a*) and size frequency data (Fig. 10*b*) obtained for the giant sea scallop (*Placopecten magellanicus*) near the Îles-de-la Madeleine, Québec (Michel Giguère, unpublished data; Giguère and Miller 1993) to illustrate the benefit of using growth data in combination with size frequency data to interpret the age composition of the frequency distributions. Estimating a growth function solely from the size frequency data in Fig. 10*b* would be frustrated by the overlap of the older age pulses and no independent information on growth or mortality. The combined analysis of size-at-age and size frequency data helps relieve this frustration (Table 3).

Despite the explicit incorporation of independent growth data into an analysis, the parameter estimates obtained are still somewhat conditional upon the analyst's choice for the largest age represented in the size frequency data. Also, annual variation in growth rate due to random climatic effects or other so-called year-effects, or Lee's phenomenon (Jones 1958), can cause an age pulse to depart (shift) from that predicted by the growth curve. This departure might appear random around an expected shift of zero, or if caused by Lee's phenomenon, might tend to be progressive in one direction as size-dependent

Fig. 10. Size-at-age (SA, $n = 640$) and size frequency (SF, $n = 1828$) data for the giant sea scallop (*Placopecten magellanicus*) with the corresponding predicted fits using each data set independently and in combination. The parameter values corresponding to the fits to these data are in Table 3.

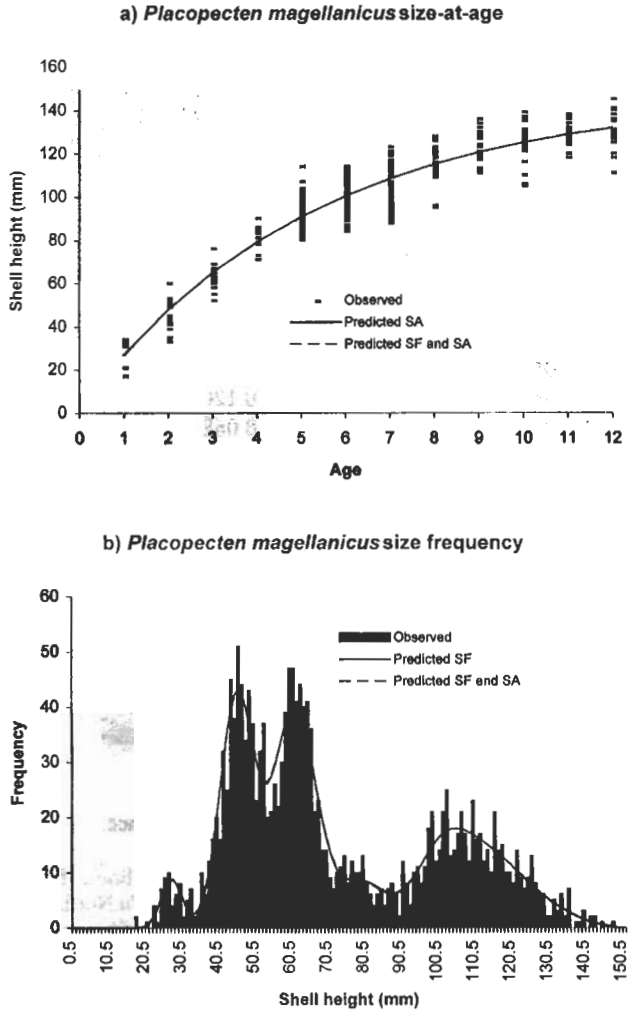

mortality persistently selects against either large or small individuals. We deal with this problem by adding a vector of parameters (ϕ_A), where A represents age. Each value of ϕ_A represents the annual shift in the mean of a discernible pulse for age A from that predicted from the pulse for the previous year ($A - 1$) and the growth curve.

If an analyst has confidence in the growth parameter estimates obtained from size-at-age or growth increment data, then a size frequency analysis can be done assisted by the independent growth data. The proportions-at-age obtained from such an analysis might then be considered as representative of the recruitment and mortality history of the age-classes recognized in the distribution although typically the confidence limits around proportions-at-age are broad. If a confident estimate of mortality, $D(l)$, can be interpreted from this recruitment and mortality history, or from another independent source, then eq. 15 can be used to calculate a value for l_x. In this example we calculated a constant value for $D(l)$ of 0.43 yr^{-1} by the method of Hoenig (1983) using our knowledge that the oldest age observed in the size-at-age data was 12 yr. We then used the value of $v = 3.2$ from the power relationship between muscle weight, the commercial product, and shell height (Giguère and Légaré 1989) to obtain an estimate for l_x of 86 mm (Table 3).

Conclusions

Scrutiny of size-at-age, growth increment, and size frequency data can be useful for developing a conceptual understanding of the interrelationships between the underlying population processes of growth and mortality in size-structured data. We therefore recommend that a careful visual interpretation of the available data be done before an analyst undertakes a formal statistical analyses of such data in order that the analyst be more prepared to judge the likelihood of success, and the conclusions, of the analyses. Further, the relative inexpense of collecting size-based data, in conjunction with a sound conceptual basis upon which to make preliminary judgments about the dynamics of growth and mortality for a fished population, can lead to the rapid implementation of simple conservation measures founded upon a reliable first impression of the population dynamics for a particular species.

We finish by cautioning readers that the data portrayed in this paper were selected and used solely for the purpose of illustrating growth and mortality patterns. Thus they, or any parameter values reported, are not necessarily those that best or completely represent the populations from which they were collected. Readers should not consider this work as a source for definitive information on the growth or mortality dynamics of those species used as examples.

Acknowledgments

This paper is a synthesis of work performed by many biologists whose contribution in data, information, and understanding is deeply appreciated. In particular we wish to thank Louise Gendron, Michel Giguère, and Jean Lambert of the Maurice Lamontagne Institute, as well as Philippe Jalbert for his original size frequency data for the waved whelk. We also wish to thank two referees of this paper, Dr. Victor Restrepo and Dr. Thomas Wainwright, and others who critically read earlier versions of this manuscript, provided advice for improvement of the manuscript, and detected and corrected errors.

References

Banks, H.T., Botsford, L.W., Kappel, F., and Wang, C. 1991. Estimation of growth and survival in size-structured cohort data: an application to larval striped bass (*Morone saxatilis*). J. Math. Biol. **30**: 125–150.

Barry, J.P., and Tegner, M.J. 1990. Inferring demographic processes from size-frequency distributions: simple models indicate specific patterns of growth and mortality. Fish. Bull. (U.S.), **88**: 13–19.

Botsford, L.W., Smith, B.D., Wing, S.R., and Quinn, J.F. 1994. Bimodality in size distributions: the red sea urchin *Strongylocentrotus franciscanus* as an example. Ecol. Appl. **4**: 42–50.

DeAngelis, D.L., and Mattice, J.S. 1979. Implications of a partial-differential-equation cohort model. Math. Biosci. **47**: 271–285.

Ebert, T.A. 1973. Estimating growth and mortality rates from size data. Oecologia, **11**: 281–298.

Fournier, D.A., and Breen, P.A. 1983. Estimation of abalone mortality rates with growth analysis. Trans. Am. Fish. Soc. **112**: 403–411.

Table 3. Formally estimated parameter values associated with the pulsed recruitment example, the giant sea scallop (*Placopecten magellanicus*).

	μ_L	σ_L	μ_K	σ_K	b	A_0	A_0'	l_x
Growth rate parameters (size-at-age data only)	147.0	7.1	0.19	2.0×10^{-2}		–0.07		86
Growth rate parameters (size-at-age and size frequency data combined)	147.6	6.8	0.19	2.0×10^{-2}		–0.08	–0.08	86

Age-class descriptions from size frequency analysis

Age	Mean	SD	Annual mean shift (ϕ_A)	Proportions
1	27.2	2.9	0*	
2	45.2	4.7	–2.6	
3	60.9	5.9	–3.9	
4	79.0	6.6	0*	
5	90.7	7.1	0*	
6	100.4	7.3	0*	
7	108.4	7.4	0*	
8	115.0	7.4	0*	
9	120.5	7.4	0*	
10	125.1	7.3	0*	
11	128.9	7.2	0*	
12	132.0	7.1	0*	

Note: All size dimensions are millimeters. The "Annual mean shift" refers to the difference in growth during one year as predicted by the growth curve and the growth represented by the size frequency data. The values for l_x were calculated using $D(l) = 0.43\ \text{yr}^{-1}$ (see text) and $\upsilon = 3.1$. An asterisk (*) beside a number indicates the number tended toward that boundary value and was subsequently fixed at that value to increase model parsimony. A dash (—) indicates that the parameter does not play a role in that particular analysis. Plots corresponding to these data are in Fig. 10.

Francis, R.I.C.C. 1988. Are growth parameters from tagging and age-length data comparable? Can. J. Fish. Aquat. Sci. **45**: 936-942.

Gendron, L. 1992. Determination of the size at sexual maturity of the waved whelk *Buccinum undatum* Linnaeus, 1758, in the Gulf of St. Lawrence, as a basis for the establishment of a minimum catchable size. J. Shellfish Res. **11**: 1–7.

Giguère, M., and Légaré, B. 1989. Exploitation du pétoncle aux Îles-de-la Madeleine en 1988. Canadian Atlantic Fisheries Scientific Advisory Committee, Dartmouth, Nova Scotia. Res. Doc. 89/14. 32 p.

Giguère, M., and Miller, R. 1993. Review of scallop fisheries in Québec. Can. Ind. Rep. Fish. Aquat. Sci. 217. 23 p.

Gulland, J.A. 1983. Fish stock assessment. A manual of basic methods. FAO/Wiley Series on Food and Agriculture. John Wiley & Sons, Toronto, Ont. 223 p.

Hilborn, R., and Walters, C.J. 1992. Quantitative fish stock assessment: choice, dynamics and uncertainty. Routledge, Chapman and Hall, Inc., New York, N.Y. 570 p.

Hoenig, J.M. 1983. Empirical use of longevity data to estimate mortality rates. Fish. Bull. (U.S.), **82**: 898–903.

Hoenig, J.M. 1987. Estimation of growth and mortality parameters for use in length-structured stock production models. *In* Length-based methods in fisheries research. ICLARM Conference Proceedings 13. *Edited by* D. Pauly and G.R. Morgan. Int. Cent. Living Aquat. Resourc. Manage., Manila, Philippines, and Kuwait Inst. Sci. Res., Safat, Kuwait. pp. 121–128.

Huston, M.A., and DeAngelis, D.L. 1987. Size bimodality in monospecific populations: a critical review of potential mechanisms. Am. Nat. **129**: 678–707.

Jalbert, P., Himmelman, J.H., Béland, P., and Thomas, B. 1989. Whelks (*Buccinum undatum*) and other subtidal invertebrate predators in the northern Gulf of St. Lawrence. Nat. Can. (Ottawa), **116**: 1–15.

Jamieson, G.S. 1986. A perspective on invertebrate fisheries management — the British Columbia experience. *In* North Pacific Workshop on stock assessment and management of invertebrates. *Edited by* G.S. Jamieson and N. Bourne. Can. Spec. Publ. Fish. Aquat. Sci. 92. pp. 57–74.

Jones, R., 1958. Lee's phenomenon of "apparent change in growth rate," with particular reference to haddock and plaice. Int. Comm. Northwest Atl. Fish. Spec. Publ. 1. pp. 229–242.

Kalvass, P., Taniguchi, I., Buttolph, P., and DeMartini, J. 1991. Relative abundance and size composition of red sea urchin, *Strongylocentrotus franciscanus*, populations along the Mendocino and Sonoma County coasts, 1989. Cal. Fish Game Administrative Rep. 91-3. 103 p.

Kato, S., and Schroeter, S.C. 1985. Biology of the red sea urchin, *Strongylocentrotus franciscanus*, and its fishery in California. Mar. Fish. Rev. **47**(3): 1–20.

Pauly, D., 1984. Fish population dynamics in tropical waters: a manual for use with programmable calculators. ICLARM Studies and Reviews 8. Int. Cent. Living Aquat. Resourc. Manage., Manila, Philippines. 325 p.

Pauly, D., and Morgan, G.R. (*Editors*). 1987. Length-based methods in fisheries research. ICLARM Conference Proceedings 13. Int. Cent. Living Aquat. Resourc. Manage., Manila, Philippines, and Kuwait Inst. Sci. Res., Safat, Kuwait. 486 p.

Pope, J.G. 1972. An investigation of the accuracy of virtual population analysis using cohort analysis. Int. Comm. Northwest Atl. Fish. Res. Bull. **9**: 65–74.

Ricker, W.E. 1975. Computation and interpretation of biological statistics of fish populations. Bull. Fish. Res. Board Can. 191. 382 p.

Sainsbury, K.J. 1980. Effect of individual variability on the von Bertalanffy growth equation. Can. J. Fish. Aquat. Sci. **37**: 241–247.

Schnute. J. 1981. A versatile growth model with statistically stable parameters. Can. J. Fish. Aquat. Sci. **38**: 1128–1140.

Schnute, J., and Fournier, D.A. 1980. A new approach to length frequency analysis: growth structure. Can. J. Fish. Aquat. Sci. **37**: 1337–1351.

Smith, B.D., and McFarlane, G.A. 1990. Growth analysis of Strait of Georgia lingcod by use of length-frequency and length-increment data in combination. Trans. Am. Fish. Soc. **119**: 802–812.

Smith, B.D., Botsford, L.W., Wing, S.R., and Quinn, J.F. 1998. Estimation of growth and mortality parameters from size frequency distributions lacking age patterns: an application to the red sea urchin (*Strongylocentrotus franciscanus*). *In* Proceedings of the North Pacific Symposium on Invertebrate Stock Assessment and Management. *Edited by* G.S. Jamieson and A. Campbell. Can. Spec. Publ. Fish. Aquat. Sci. 125. (Unpublished.)

Tegner M.J., and Levin, L.A. 1983. Spiny lobsters and sea urchins: analysis of a predator–prey interaction. J. Exp. Mar. Biol. Ecol. **73**: 125–150.

Van Sickle, J. 1977. Mortality rates from size distributions. Oecologia, **27**: 311–318.

von Foerster, H. 1959. Some remarks on changing populations. *In* The kinetics of cell proliferation. *Edited by* F. Stahlman. Grune and Stratton, New York, N.Y. pp. 382–407.